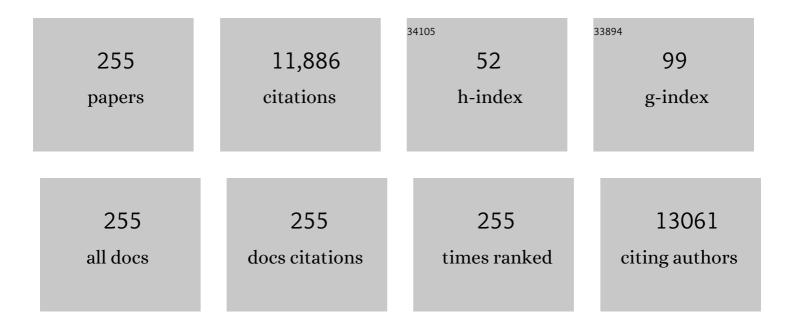
## Jehad K El-Demellawi

List of Publications by Year in descending order

Source: https://exaly.com/author-pdf/5617357/publications.pdf Version: 2024-02-01



#	Article	IF	CITATIONS
1	A novel metal–organic frameworkâ€derived NiSe <sub>2</sub> /ZnSeâ€NC as advanced anode materials for highâ€performance asymmetric supercapacitors. Electrochemical Science Advances, 2022, 2, e2100047.	2.8	8
2	Hotspots, frontiers, and emerging trends of tandem solar cell research: A comprehensive review. International Journal of Energy Research, 2022, 46, 104-123.	4.5	12
3	n-type absorber by Cd2+ doping achieves high-performance carbon-based CsPbIBr2 perovskite solar cells. Journal of Colloid and Interface Science, 2022, 608, 40-47.	9.4	30
4	Enhancing efficiency of perovskite solar cells from surface passivation of Co2+ doped CuGaO2 nanocrystals. Journal of Colloid and Interface Science, 2022, 607, 1280-1286.	9.4	11
5	Rear Interface Engineering to Suppress Migration of Iodide Ions for Efficient Perovskite Solar Cells with Minimized Hysteresis. Advanced Functional Materials, 2022, 32, 2107823.	14.9	57
6	Efficient and Stable Carbonâ€Based CsPbIBr <sub>2</sub> Perovskite Solar Cells by 4â€Aminomethyltetrahydropyran Acetate Modification. Advanced Materials Interfaces, 2022, 9, 2101463.	3.7	11
7	Porous Ti <sub>3</sub> C <sub>2</sub> T <sub><i>x</i></sub> MXene Membranes for Highly Efficient Salinity Gradient Energy Harvesting. ACS Nano, 2022, 16, 792-800.	14.6	60
8	Simultaneously Mitigating Anion and Cation Defects Both in Bulk and Interface for Highâ€Effective Perovskite Solar Cells. Solar Rrl, 2022, 6, .	5.8	2
9	Face-on oriented hydrophobic conjugated polymers as dopant-free hole-transport materials for efficient and stable perovskite solar cells with a fill factor approaching 85%. Journal of Materials Chemistry A, 2022, 10, 3409-3417.	10.3	19
10	Interlayer Modification Using Phenylethylamine Tetrafluoroborate for Highly Effective Perovskite Solar Cells. ACS Applied Energy Materials, 2022, 5, 658-666.	5.1	8
11	5â€Chloroindole as Interface Modifier to Improve the Efficiency and Stability of Planar Perovskite Solar Cells. Solar Rrl, 2022, 6, .	5.8	9
12	MXene-Coated Membranes for Autonomous Solar-Driven Desalination. ACS Applied Materials & Interfaces, 2022, 14, 5265-5274.	8.0	57
13	Bulky ammonium iodide and in-situ formed 2D Ruddlesden-Popper layer enhances the stability and efficiency of perovskite solar cells. Journal of Colloid and Interface Science, 2022, 614, 247-255.	9.4	12
14	Scaled Deposition of Ti <sub>3</sub> C <sub>2</sub> <i>T</i> <sub><i>x</i></sub> MXene on Complex Surfaces: Application Assessment as Rear Electrodes for Silicon Heterojunction Solar Cells. ACS Nano, 2022, 16, 2419-2428.	14.6	28
15	Zinc and Acetate Co-doping for Stable Carbon-Based CsPbIBr <sub>2</sub> Solar Cells with Efficiency over 10.6%. ACS Applied Energy Materials, 2022, 5, 2720-2726.	5.1	4
16	Interfacial Defect Passivation Effect of <i>N</i> -Methyl- <i>N</i> -(thien-2-ylmethyl)amine for Highly Effective Perovskite Solar Cells. ACS Applied Energy Materials, 2022, 5, 4270-4278.	5.1	2
17	High-efficiency and ultraviolet stable carbon-based CsPbIBr2 solar cells from single crystal three-dimensional anatase titanium dioxide nanoarrays with ultraviolet light shielding function. Journal of Colloid and Interface Science, 2022, 616, 201-209.	9.4	9
18	Selfâ€Activation Enables Cationic and Anionic Coâ€Storage in Organic Frameworks. Advanced Energy Materials, 2022, 12, .	19.5	11

#	Article	IF	CITATIONS
19	Multifunctional Molecule Modification toward Efficient Carbonâ€Based Allâ€Inorganic CsPblBr <sub>2</sub> Perovskite Solar Cells. Advanced Sustainable Systems, 2022, 6, .	5.3	15
20	Single-crystalline TiO2 nanoparticles for stable and efficient perovskite modules. Nature Nanotechnology, 2022, 17, 598-605.	31.5	121
21	Plasmonic Nb <sub>2</sub> C <i>T</i> <sub><i>x</i></sub> MXene-MAPbI <sub>3</sub> Heterostructure for Self-Powered Visible-NIR Photodiodes. ACS Nano, 2022, 16, 7904-7914.	14.6	19
22	4-Hydroxy-2,2,6,6-tetramethylpiperidine as a Bifunctional Interface Modifier for High-Efficiency and Stable Perovskite Solar Cells. ACS Applied Energy Materials, 2022, 5, 6754-6763.	5.1	3
23	Performance Improvement of Planar Perovskite Solar Cells Using Lauric Acid as Interfacial Modifier. ACS Applied Energy Materials, 2022, 5, 8501-8509.	5.1	2
24	Polarized Molecule 4-(Aminomethyl) Benzonitrile Hydrochloride for Efficient and Stable Perovskite Solar Cells. ACS Applied Materials & Interfaces, 2022, 14, 33383-33391.	8.0	7
25	High thermally stable hybrid materials based on amorphous porous silicon nanoparticles and imidazolium-based ionic liquids: Structural and chemical analysis. Materials Today: Proceedings, 2021, 39, 1132-1140.	1.8	0
26	Guanidinium iodide modification enabled highly efficient and stable all-inorganic CsPbBr3 perovskite solar cells. Electrochimica Acta, 2021, 365, 137360.	5.2	27
27	Enhanced photovoltage and stability of perovskite photovoltaics enabled by a cyclohexylmethylammonium iodide-based 2D perovskite passivation layer. Nanoscale, 2021, 13, 14915-14924.	5.6	16
28	Ti <sub>3</sub> C <sub>2</sub> T <sub><i>x</i></sub> MXene-Activated Fast Gelation of Stretchable and Self-Healing Hydrogels: A Molecular Approach. ACS Nano, 2021, 15, 2698-2706.	14.6	157
29	Postpassivation of Cs <sub>0.05</sub> (FA <sub>0.83</sub> MA <sub>0.17</sub> ) <sub>0.95</sub> Pb(I <sub>0.83</sub> Br <sub>C Perovskite Films with Tris(pentafluorophenyl)borane. ACS Applied Materials &amp; Interfaces, 2021, 13, 2472-2482.</sub>	.17 8.0	) <sub>3</sub>
30	Highly efficient and stable planar perovskite solar cells with K <sub>3</sub> [Fe(CN) <sub>6</sub> ]-doped spiro-OMeTAD. Journal of Materials Chemistry C, 2021, 9, 7726-7733.	5.5	20
31	The Impact of PbI 2 :KI Alloys on the Performance of Sequentially Deposited Perovskite Solar Cells. European Journal of Inorganic Chemistry, 2021, 2021, 821-830.	2.0	5
32	Supermolecule Cucurbituril Subnanoporous Carbon Supercapacitor (SCSCS). Nano Letters, 2021, 21, 2156-2164.	9.1	40
33	Engineering Bandâ€Type Alignment in CsPbBr <sub>3</sub> Perovskiteâ€Based Artificial Multiple Quantum Wells. Advanced Materials, 2021, 33, e2005166.	21.0	12
34	In Situ Interface Engineering with a Spiroâ€OMeTAD/CoO Hierarchical Structure via Oneâ€5tep Spin oating for Efficient and Stable Perovskite Solar Cells. Advanced Materials Interfaces, 2021, 8, 2002041.	3.7	2
35	Additive Engineering by 6-Aminoquinoline Monohydrochloride for High-Performance Perovskite Solar Cells. ACS Applied Energy Materials, 2021, 4, 7083-7090.	5.1	9
36	Carbon-Based Stable CsPbIBr <sub>2</sub> Solar Cells with Efficiency of over 10% from Bifunctional Quinoline Sulfate Modification. ACS Applied Energy Materials, 2021, 4, 5747-5755.	5.1	13

#	Article	IF	CITATIONS
37	Hotspots, Frontiers, and Emerging Trends of Superabsorbent Polymer Research: A Comprehensive Review. Frontiers in Chemistry, 2021, 9, 688127.	3.6	14
38	Highâ€Efficiency Carbonâ€Based CsPbIBr <sub>2</sub> Solar Cells with Interfacial Energy Loss Suppressed by a Thin Bulkâ€Heterojunction Layer. Solar Rrl, 2021, 5, 2100375.	5.8	30
39	Efficient and Stable 2D@3D/2D Perovskite Solar Cells Based on Dual Optimization of Grain Boundary and Interface. ACS Energy Letters, 2021, 6, 3614-3623.	17.4	113
40	Alkali Metal Fluoride-Modified Tin Oxide for n–i–p Planar Perovskite Solar Cells. ACS Applied Materials & Interfaces, 2021, 13, 50083-50092.	8.0	12
41	Phthalide and 1â€юdooctadecane Synergistic Optimization for Highly Efficient and Stable Perovskite Solar Cells. Small, 2021, 17, e2103336.	10.0	23
42	Defect Passivation through Cyclohexylethylamine Post-treatment for High-Performance and Stable Perovskite Solar Cells. ACS Applied Energy Materials, 2021, 4, 12848-12857.	5.1	6
43	Surface Reconstruction and In Situ Formation of 2D Layer for Efficient and Stable 2D/3D Perovskite Solar Cells. Small Methods, 2021, 5, e2101000.	8.6	33
44	High-Performance Perovskite Solar Cells by Doping Didodecyl Dimethyl Ammonium Bromide in the Hole Transport Layer. ACS Applied Energy Materials, 2021, 4, 13471-13481.	5.1	2
45	Ammonium Fluoride Interface Modification for Highâ€Performance and Longâ€Term Stable Perovskite Solar Cells. Energy Technology, 2020, 8, 1901017.	3.8	12
46	Synergy of Plasmonic Silver Nanorod and Water for Enhanced Planar Perovskite Photovoltaic Devices. Solar Rrl, 2020, 4, 1900231.	5.8	26
47	Regulation of Interfacial Charge Transfer and Recombination for Efficient Planar Perovskite Solar Cells. Solar Rrl, 2020, 4, 1900198.	5.8	46
48	CoBr <sub>2</sub> -doping-induced efficiency improvement of CsPbBr <sub>3</sub> planar perovskite solar cells. Journal of Materials Chemistry C, 2020, 8, 1649-1655.	5.5	37
49	Efficient mesoscopic perovskite solar cells from emulsion-based bottom-up self-assembled TiO2 microspheres. Journal of Materials Science: Materials in Electronics, 2020, 31, 1969-1975.	2.2	0
50	Suppressing Vacancy Defects and Grain Boundaries via Ostwald Ripening for Highâ€Performance and Stable Perovskite Solar Cells. Advanced Materials, 2020, 32, e1904347.	21.0	172
51	Highly efficient tin perovskite solar cells achieved in a wide oxygen concentration range. Journal of Materials Chemistry A, 2020, 8, 2760-2768.	10.3	85
52	Single Source, Surfactantâ€Free, and Oneâ€Step Solvothermal Route Synthesized TiO <sub>2</sub> Microspheres for Highly Efficient Mesoscopic Perovskite Solar Cells. Solar Rrl, 2020, 4, 2000519.	5.8	7
53	Autonomous MXene-PVDF actuator for flexible solar trackers. Nano Energy, 2020, 77, 105277.	16.0	35
54	Strong electron acceptor additive based spiro-OMeTAD for high-performance and hysteresis-less planar perovskite solar cells. RSC Advances, 2020, 10, 38736-38745.	3.6	12

#	Article	IF	CITATIONS
55	MXene hydrogels: fundamentals and applications. Chemical Society Reviews, 2020, 49, 7229-7251.	38.1	368
56	Additive Engineering by Bifunctional Guanidine Sulfamate for Highly Efficient and Stable Perovskites Solar Cells. Small, 2020, 16, e2004877.	10.0	35
57	Building Lithiophilic Ion onduction Highways on Garnetâ€Type Solidâ€5tate Li <sup>+</sup> Conductors. Advanced Energy Materials, 2020, 10, 1904230.	19.5	62
58	Unprecedented Surface Plasmon Modes in Monoclinic MoO <sub>2</sub> Nanostructures. Advanced Materials, 2020, 32, e1908392.	21.0	28
59	MXene Printing and Patterned Coating for Device Applications. Advanced Materials, 2020, 32, e1908486.	21.0	239
60	Defect Control Strategy by Bifunctional Thioacetamide at Low Temperature for Highly Efficient Planar Perovskite Solar Cells. ACS Applied Materials & Interfaces, 2020, 12, 12883-12891.	8.0	24
61	T-ZnOw/ZnONP Double-Layer Composite Photoanode with One-Dimensional Low-Resistance Photoelectron Channels for High-Efficiency DSSCs. Journal of Physical Chemistry C, 2020, 124, 4408-4413.	3.1	3
62	Highly Efficient CsPbBr <sub>3</sub> Planar Perovskite Solar Cells via Additive Engineering with NH <sub>4</sub> SCN. ACS Applied Materials & Interfaces, 2020, 12, 10579-10587.	8.0	80
63	Polymeric Sulfur as a Li Ion Conductor. Nano Letters, 2020, 20, 2191-2196.	9.1	15
64	Highâ€Efficiency Lowâ€Temperatureâ€Processed Mesoscopic Perovskite Solar Cells from SnO <sub>2</sub> Nanorod Selfâ€Assembled Microspheres. Solar Rrl, 2020, 4, 1900558.	5.8	21
65	Highâ€Performance Perovskite Solar Cells Using Iodine as Effective Dopant for Spiroâ€OMeTAD. Energy Technology, 2020, 8, 1901171.	3.8	14
66	Fluoroaromatic Cationâ€Assisted Planar Junction Perovskite Solar Cells with Improved <i>V</i> <sub>OC</sub> and Stability: The Role of Fluorination Position. Solar Rrl, 2020, 4, 2000107.	5.8	68
67	MXene improves the stability and electrochemical performance of electropolymerized PEDOT films. APL Materials, 2020, 8, .	5.1	25
68	Inkjet-printed Ti <sub>3</sub> C <sub>2</sub> T <sub>x</sub> MXene electrodes for multimodal cutaneous biosensing. JPhys Materials, 2020, 3, 044004.	4.2	30
69	Efficient inverted planar perovskite solar cells based on inorganic hole-transport layers from nickel-containing organic sol. Functional Materials Letters, 2019, 12, 1850088.	1.2	7
70	Synergistic Cobalt Sulfide/Eggshell Membrane Carbon Electrode. ACS Applied Materials & Interfaces, 2019, 11, 32244-32250.	8.0	32
71	Toward Highly Reproducible, Efficient, and Stable Perovskite Solar Cells via Interface Engineering with CoO Nanoplates. ACS Applied Materials & Interfaces, 2019, 11, 32159-32168.	8.0	41
72	Metal Halide Perovskite and Phosphorus Doped g-C <sub>3</sub> N <sub>4</sub> Bulk Heterojunctions for Air-Stable Photodetectors. ACS Energy Letters, 2019, 4, 2315-2322.	17.4	36

#	Article	IF	CITATIONS
73	Visible light-driven flower-like Bi/BiOClxBr(1â^'x) heterojunction with excellent photocatalytic performance. Journal of the Iranian Chemical Society, 2019, 16, 2743-2754.	2.2	7
74	Solvent engineering of LiTFSI towards high-efficiency planar perovskite solar cells. Solar Energy, 2019, 194, 321-328.	6.1	17
75	MAPbl <sub>3</sub> Single Crystals Free from Hole-Trapping Centers for Enhanced Photodetectivity. ACS Energy Letters, 2019, 4, 2579-2584.	17.4	40
76	A high-performance asymmetric supercapacitor based on Ni <sub>3</sub> S <sub>2</sub> -coated NiSe arrays as positive electrode. New Journal of Chemistry, 2019, 43, 2389-2399.	2.8	41
77	Improved photovoltaic performance of perovskite solar cells by utilizing down-conversion NaYF <sub>4</sub> :Eu <sup>3+</sup> nanophosphors. Journal of Materials Chemistry C, 2019, 7, 937-942.	5.5	40
78	MXenes for Plasmonic Photodetection. Advanced Materials, 2019, 31, e1807658.	21.0	175
79	High performance and stable perovskite solar cells using vanadic oxide as a dopant for spiro-OMeTAD. Journal of Materials Chemistry A, 2019, 7, 13256-13264.	10.3	81
80	Pyrrole: an additive for improving the efficiency and stability of perovskite solar cells. Journal of Materials Chemistry A, 2019, 7, 11764-11770.	10.3	61
81	A C <sub>60</sub> /TiO <sub>x</sub> bilayer for conformal growth of perovskite films for UV stable perovskite solar cells. Journal of Materials Chemistry A, 2019, 7, 11086-11094.	10.3	64
82	Polymer Electrolyte Glue: A Universal Interfacial Modification Strategy for All-Solid-State Li Batteries. Nano Letters, 2019, 19, 2343-2349.	9.1	105
83	Hollow rod-like hybrid Co2CrO4/Co1â^'xS for high-performance asymmetric supercapacitor. Journal of Materials Science: Materials in Electronics, 2019, 30, 1045-1055.	2.2	4
84	Low-temperature solution-processing high quality Nb-doped SnO <sub>2</sub> nanocrystals-based electron transport layers for efficient planar perovskite solar cells. Functional Materials Letters, 2019, 12, 1850091.	1.2	21
85	High-Performance and Hysteresis-Free Perovskite Solar Cells Based on Rare-Earth-Doped SnO <sub>2</sub> Mesoporous Scaffold. Research, 2019, 2019, 4049793.	5.7	35
86	Preparation of MnO2/porous carbon material with core–shell structure and its application in supercapacitor. Journal of Materials Science: Materials in Electronics, 2018, 29, 7957-7964.	2.2	6
87	Cadmium sulfide as an efficient electron transport material for inverted planar perovskite solar cells. Chemical Communications, 2018, 54, 3170-3173.	4.1	41
88	Hydrothermal Synthesis of Hybrid Rod‣ike Hollow CoWO <sub>4</sub> /Co <sub>1â^'<i>x</i></sub> S for Highâ€Performance Supercapacitors. ChemElectroChem, 2018, 5, 1047-1055.	3.4	30
89	Growth of Ni3Se2 nanosheets on Ni foam for asymmetric supercapacitors. Journal of Materials Science: Materials in Electronics, 2018, 29, 4649-4657.	2.2	33
90	Annealingâ€Free Cr <sub>2</sub> O <sub>3</sub> Electronâ€Selective Layer for Efficient Hybrid Perovskite Solar Cells. ChemSusChem, 2018, 11, 619-628.	6.8	22

6

#	Article	IF	CITATIONS
91	Improving the Performance of a Perovskite Solar Cell by Adjusting the Dispersant for Titanium Dioxide. Energy Technology, 2018, 6, 677-682.	3.8	2
92	Improved performance of a CoTe//AC asymmetric supercapacitor using a redox additive aqueous electrolyte. RSC Advances, 2018, 8, 7997-8006.	3.6	63
93	CdSe x S1â^'x /CdS-cosensitized 3D TiO2 hierarchical nanostructures for efficient energy conversion. Journal of Solid State Electrochemistry, 2018, 22, 347-353.	2.5	7
94	Construction of NiTe/NiSe Composites on Ni Foam for Highâ€Performance Asymmetric Supercapacitor. ChemElectroChem, 2018, 5, 507-514.	3.4	36
95	Multipolar Surface Plasmons in 2D Ti3C2Tx Flakes: an Ultra-High Resolution EELS with Conventional TEM and In-Situ Heating Study. Microscopy and Microanalysis, 2018, 24, 1578-1579.	0.4	4
96	An Additive of Sulfonic Lithium Salt for Highâ€Performance Perovskite Solar Cells. ChemistrySelect, 2018, 3, 12320-12324.	1.5	8
97	Dual interfacial modification engineering with p-type NiO nanocrystals for preparing efficient planar perovskite solar cells. Journal of Materials Chemistry C, 2018, 6, 13034-13042.	5.5	37
98	Thiourea Interfacial Modification for Highly Efficient Planar Perovskite Solar Cells. ACS Applied Energy Materials, 2018, 1, 6700-6706.	5.1	20
99	Diboronâ€Assisted Interfacial Defect Control Strategy for Highly Efficient Planar Perovskite Solar Cells. Advanced Materials, 2018, 30, e1805085.	21.0	128
100	Giant Photoluminescence Enhancement in CsPbCl <sub>3</sub> Perovskite Nanocrystals by Simultaneous Dual-Surface Passivation. ACS Energy Letters, 2018, 3, 2301-2307.	17.4	244
101	N,Oâ€Codoped Hierarchically Porous Carbons Derived from Squid Pen for Highâ€Capacity Supercapacitors. ChemistrySelect, 2018, 3, 8144-8150.	1.5	4
102	An efficient solvent additive for the preparation of anion-cation-mixed hybrid and the high performance perovskite solar cells. Journal of Colloid and Interface Science, 2018, 531, 602-608.	9.4	15
103	High-Efficiency Planar Hybrid Perovskite Solar Cells Using Indium Sulfide as Electron Transport Layer. ACS Applied Energy Materials, 2018, 1, 4050-4056.	5.1	30
104	Tunable Multipolar Surface Plasmons in 2D Ti <sub>3</sub> C <sub>2</sub> <i>T</i> <sub><i>x</i></sub> MXene Flakes. ACS Nano, 2018, 12, 8485-8493.	14.6	179
105	Low-temperature sintered SnO2 electron transport layer for efficient planar perovskite solar cells. Journal of Materials Science: Materials in Electronics, 2018, 29, 13138-13147.	2.2	12
106	Low-temperature solution-processed efficient electron-transporting layers based on BF <sub>4</sub> <sup>â^'</sup> -capped TiO <sub>2</sub> nanorods for high-performance planar perovskite solar cells. Journal of Materials Chemistry C, 2018, 6, 334-341.	5.5	31
107	Solvent engineering for forming stonehenge-like PbI <sub>2</sub> nano-structures towards efficient perovskite solar cells. Journal of Materials Chemistry A, 2017, 5, 4376-4383.	10.3	59
108	Fabrication of ZnO/SnO2 hierarchical structures as the composite photoanodes for efficient CdS/CdSe co-sensitized solar cells. Applied Physics A: Materials Science and Processing, 2017, 123, 1.	2.3	3

#	Article	IF	CITATIONS
109	Nickel selenide/reduced graphene oxide nanocomposite as counter electrode for high efficient dye-sensitized solar cells. Journal of Colloid and Interface Science, 2017, 498, 217-222.	9.4	41
110	Fabrication a thin nickel oxide layer on photoanodes for control of charge recombination in dye-sensitized solar cells. Journal of Solid State Electrochemistry, 2017, 21, 1523-1531.	2.5	7
111	Hybrid electrolytes based on ionic liquids and amorphous porous silicon nanoparticles: Organization and electrochemical properties. Applied Materials Today, 2017, 9, 10-20.	4.3	16
112	Modulated CH3NH3PbI3â^'xBrx film for efficient perovskite solar cells exceeding 18%. Scientific Reports, 2017, 7, 44603.	3.3	60
113	Counter electrodes in dye-sensitized solar cells. Chemical Society Reviews, 2017, 46, 5975-6023.	38.1	609
114	CH <sub>3</sub> NH <sub>3</sub> Br Additive for Enhanced Photovoltaic Performance and Air Stability of Planar Perovskite Solar Cells prepared by Two‣tep Dipping Method. Energy Technology, 2017, 5, 1887-1894.	3.8	18
115	A gradient engineered hole-transporting material for monolithic series-type large-area perovskite solar cells. Journal of Materials Chemistry A, 2017, 5, 21161-21168.	10.3	35
116	Addition of Lithium Iodide into Precursor Solution for Enhancing the Photovoltaic Performance of Perovskite Solar Cells. Energy Technology, 2017, 5, 1814-1819.	3.8	4
117	Interface Engineering of electron Transport Layerâ€Free Planar Perovskite Solar Cells with Efficiency Exceeding 15 %. Energy Technology, 2017, 5, 1844-1851.	3.8	13
118	Tuning the Fermi Level of TiO <sub>2</sub> Electron Transport Layer through Europium Doping for Highly Efficient Perovskite Solar Cells. Energy Technology, 2017, 5, 1820-1826.	3.8	42
119	Synthesis and Characterization of Luminescent Amorphous Porous Silicon (ap-Si) Nanoparticles via unconventional Stain Etching. Journal of Physics: Conference Series, 2016, 758, 012018.	0.4	1
120	Facile synthesis of porous CuS film as a high efficient counter electrode for quantum-dot-sensitized solar cells. Applied Physics A: Materials Science and Processing, 2016, 122, 1.	2.3	1
121	Synthesis and gas sensing properties of SnO2 nanoparticles with different morphologies. Journal of Porous Materials, 2016, 23, 1189-1196.	2.6	8
122	High-Performance Molybdenum Diselenide Electrodes Used in Dye-Sensitized Solar Cells and Supercapacitors. IEEE Journal of Photovoltaics, 2016, 6, 1196-1202.	2.5	24
123	Multifunctional Rareâ€Earthâ€Doped Tin Oxide Compact Layers for Improving Performances of Photovoltaic Devices. Advanced Materials Interfaces, 2016, 3, 1600881.	3.7	16
124	Optimization of CdSe layer on modified ZnO hierarchical spheres by spin-SILAR for efficient CdS/CdSe co-sensitized solar cells. Journal of Materials Science: Materials in Electronics, 2016, 27, 6656-6664.	2.2	4
125	An efficient method to prepare high-performance dye-sensitized photoelectrodes using ordered TiO2 nanotube arrays and TiO2 quantum dot blocking layers. Journal of Solid State Electrochemistry, 2016, 20, 2643-2650.	2.5	13
126	Mesoporous Co0.85Se nanosheets supported on Ni foam as a positive electrode material for asymmetric supercapacitor. Applied Surface Science, 2016, 362, 469-476.	6.1	83

#	Article	IF	CITATIONS
127	Preparation of long persistent phosphor SrAl2O4:Eu2+, Dy3+ and its application in dye-sensitized solar cells. Journal of Materials Science: Materials in Electronics, 2016, 27, 1350-1356.	2.2	25
128	High-performance and transparent counter electrodes based on polypyrrole and ferrous sulfide nanoparticles for dye-sensitized solar cells. Journal of Materials Science: Materials in Electronics, 2016, 27, 5680-5685.	2.2	8
129	High-performance Pt-NiO nanosheet-based counter electrodes for dye-sensitized solar cells. Journal of Solid State Electrochemistry, 2016, 20, 759-766.	2.5	21
130	An efficient titanium foil based perovskite solar cell: using a titanium dioxide nanowire array anode and transparent poly(3,4-ethylenedioxythiophene) electrode. RSC Advances, 2016, 6, 2778-2784.	3.6	51
131	An in situ polymerized PEDOT/Fe <sub>3</sub> O <sub>4</sub> composite as a Pt-free counter electrode for highly efficient dye sensitized solar cells. RSC Advances, 2016, 6, 1637-1643.	3.6	28
132	Oxidation Induced Giant Modulation in the Luminescence of Colloidal Amorphous Porous Silicon Nanoparticles. Materials Research Society Symposia Proceedings, 2015, 1748, 44.	0.1	0
133	Highâ€performing dyeâ€sensitized solar cells based on reduced graphene oxide/ <scp>PEDOTâ€PSS</scp> counter electrodes with sulfuric acid postâ€treatment. Journal of Applied Polymer Science, 2015, 132, .	2.6	15
134	Petal-like cobalt selenide nanosheets used as counter electrode in high efficient dye-sensitized solar cells. Journal of Materials Science: Materials in Electronics, 2015, 26, 2501-2507.	2.2	16
135	PEDOT:PSS assisted preparation of a graphene/nickel cobalt oxide hybrid counter electrode to serve in efficient dye-sensitized solar cells. RSC Advances, 2015, 5, 100159-100168.	3.6	15
136	TiO <sub>2</sub> quantum dots as superb compact block layers for high-performance CH <sub>3</sub> NH <sub>3</sub> Pbl <sub>3</sub> perovskite solar cells with an efficiency of 16.97%. Nanoscale, 2015, 7, 20539-20546.	5.6	87
137	Electrolytes in Dye-Sensitized Solar Cells. Chemical Reviews, 2015, 115, 2136-2173.	47.7	852
138	Improved photovoltaic performance of CdS/CdSe co-sensitized solar cells by using calcined starch–ZnO mesoporous spheres. Journal of Materials Science: Materials in Electronics, 2015, 26, 2955-2961.	2.2	2
139	Preparation of nano-flower-like SnO2 particles and their applications in efficient CdS quantum dots sensitized solar cells. Journal of Materials Science: Materials in Electronics, 2015, 26, 7914-7920.	2.2	10
140	Room-Temperature Reactivity Of Silicon Nanocrystals With Solvents: The Case Of Ketone And Hydrogen Production From Secondary Alcohols: Catalysis?. ACS Applied Materials & Interfaces, 2015, 7, 13794-13800.	8.0	19
141	Synthesis of hierarchical nanowires-based TiO2 spheres for their application as the light blocking layers in CdS/CdSe co-sensitized solar cells. Journal of Materials Science: Materials in Electronics, 2015, 26, 693-699.	2.2	5
142	Cadmium selenide quantum dots solar cells featuring nickel sulfide/polyaniline as efficient counter electrode provide 4.15% efficiency. RSC Advances, 2015, 5, 42101-42108.	3.6	12
143	A strategy to enhance overall efficiency for dye-sensitized solar cells with a transparent electrode of nickel sulfide decorated with poly(3,4-ethylenedioxythiophene). RSC Advances, 2015, 5, 43639-43647.	3.6	17
144	A highly efficient flexible dye-sensitized solar cell based on nickel sulfide/platinum/titanium counter electrode. Nanoscale Research Letters, 2015, 10, 1.	5.7	959

#	Article	IF	CITATIONS
145	Hydrothermal synthesis of CoMoO <sub>4</sub> /Co <sub>9</sub> S <sub>8</sub> hybrid nanotubes based on counter electrodes for highly efficient dye-sensitized solar cells. RSC Advances, 2015, 5, 83029-83035.	3.6	19
146	Facile synthesis of Ni <sub>0.85</sub> Se on Ni foam for high-performance asymmetric capacitors. RSC Advances, 2015, 5, 81474-81481.	3.6	41
147	Cobalt selenide/tin selenide hybrid used as a high efficient counter electrode for dye-sensitized solar cells. Journal of Materials Science: Materials in Electronics, 2015, 26, 10102-10108.	2.2	21
148	Preparation of PAA- <i>g</i> -PEG/PANI polymer gel electrolyte and its application in quasi solid state dye-sensitized solar cells. Polymer Engineering and Science, 2015, 55, 322-326.	3.1	18
149	Band-gap engineering by molecular mechanical strain-induced giant tuning of the luminescence in colloidal amorphous porous silicon nanostructures. Physical Chemistry Chemical Physics, 2014, 16, 25273-25279.	2.8	10
150	Nickel sulfide films with significantly enhanced electrochemical performance induced by self-assembly of 4-aminothiophenol and their application in dye-sensitized solar cells. RSC Advances, 2014, 4, 64068-64074.	3.6	18
151	A redoxâ€mediatorâ€doped gel polymer electrolyte applied in quasiâ€solidâ€state supercapacitors. Journal of Applied Polymer Science, 2014, 131, .	2.6	33
152	Influences of solvents on morphology, light absorbing ability and photovoltaic performance of Sb2S3-sensitized TiO2 photoanodes by chemical bath deposition method. Journal of Materials Science: Materials in Electronics, 2014, 25, 673-677.	2.2	4
153	Efficient Mn-doped CdS quantum dot sensitized solar cells based on SnO2 microsphere photoelectrodes. Journal of Materials Science: Materials in Electronics, 2014, 25, 754-759.	2.2	13
154	Room temperature polymerization of poly(3,4-ethylenedioxythiophene) as transparent counter electrodes for dye-sensitized solar cells. Polymers for Advanced Technologies, 2014, 25, 1560-1564.	3.2	11
155	Electrospun lead-doped titanium dioxide nanofibers and the in situ preparation of perovskite-sensitized photoanodes for use in high performance perovskite solar cells. Journal of Materials Chemistry A, 2014, 2, 16856-16862.	10.3	81
156	Improving photoelectrical performance of dye sensitized solar cells by doping Y2O3:Tb3+ nanorods. Journal of Materials Science: Materials in Electronics, 2014, 25, 2060-2065.	2.2	6
157	Bifacial illuminated PbS quantum dot-sensitized solar cells with translucent CuS counter electrodes. Journal of Materials Science: Materials in Electronics, 2014, 25, 3016-3022.	2.2	6
158	TiCl4 assisted formation of nano-TiO2 secondary structure in photoactive electrodes for high efficiency dye-sensitized solar cells. Science China Chemistry, 2014, 57, 888-894.	8.2	7
159	Template-free synthesis of polyaniline nanobelts as a catalytic counter electrode in dye-sensitized solar cells. Polymers for Advanced Technologies, 2014, 25, 343-346.	3.2	13
160	Preparation of high performance perovskite-sensitized nanoporous titanium dioxide photoanodes by in situ method for use in perovskite solar cells. Journal of Materials Chemistry A, 2014, 2, 16531-16537.	10.3	62
161	Bifacial dye-sensitized solar cells: A strategy to enhance overall efficiency based on transparent polyaniline electrode. Scientific Reports, 2014, 4, 4028.	3.3	141
162	An ultraviolet responsive hybrid solar cell based on titania/poly(3-hexylthiophene). Scientific Reports, 2013, 3, 1283.	3.3	59

#	Article	IF	CITATIONS
163	Efficiency improvement of flexible dye-sensitized solar cells by introducing mesoporous TiO2 microsphere. Science China Chemistry, 2013, 56, 1470-1477.	8.2	6
164	A dye-sensitized solar cell based on PEDOT:PSS counter electrode. Science Bulletin, 2013, 58, 559-566.	1.7	36
165	A high performance Pt-free counter electrode of nickel sulfide/multi-wall carbon nanotube/titanium used in dye-sensitized solar cells. Journal of Materials Chemistry A, 2013, 1, 13885.	10.3	89
166	High performance platinum-free counter electrode of molybdenum sulfide–carbon used in dye-sensitized solar cells. Journal of Materials Chemistry A, 2013, 1, 1495-1501.	10.3	185
167	Quantum dot-sensitized solar cells employing Pt/C60 counter electrode provide an efficiency exceeding 2%. Science China Chemistry, 2013, 56, 93-100.	8.2	5
168	Application of poly(3,4-ethylenedioxythiophene):polystyrenesulfonate in polymer heterojunction solar cells. Journal of Materials Science, 2013, 48, 3528-3534.	3.7	8
169	Pulse electrodeposition of CoS on MWCNT/Ti as a high performance counter electrode for a Pt-free dye-sensitized solar cell. Journal of Materials Chemistry A, 2013, 1, 1289-1295.	10.3	95
170	Dual functions of YF3:Eu3+ for improving photovoltaic performance of dye-sensitized solar cells. Scientific Reports, 2013, 3, 2058.	3.3	80
171	A HIGH EFFICIENCY DYE-SENSITIZED SOLAR CELL WITH NANO-TIO2 SECONDARY STRUCTURE IN THE PHOTOANODE. Functional Materials Letters, 2013, 06, 1350014.	1.2	4
172	LARGE-SIZED DYE-SENSITIZED SOLAR CELLS WITH <font>TiO<sub>2</sub></font> CEMENTED AND PROTECTED SILVER GRIDS. Functional Materials Letters, 2012, 05, 1250010.	1.2	1
173	Preparation of hierarchical tin oxide microspheres and their application in dye-sensitized solar cells. Journal of Materials Chemistry, 2012, 22, 25335.	6.7	35
174	High efficient PANI/Pt nanofiber counter electrode used in dye-sensitized solar cell. RSC Advances, 2012, 2, 4062.	3.6	42
175	p–n Heterojunction on dye-sensitized ZnO nanorod arrays and macroporous polyaniline network. RSC Advances, 2012, 2, 1863.	3.6	19
176	Controllably hierarchical growth of large-scale ZnO microrods. RSC Advances, 2012, 2, 2211.	3.6	3
177	A simple and high-effective electrolyte mediated with p-phenylenediamine for supercapacitor. Journal of Materials Chemistry, 2012, 22, 19025.	6.7	154
178	Pulse electropolymerization of high performance PEDOT/MWCNT counter electrodes for Pt-free dye-sensitized solar cells. Journal of Materials Chemistry, 2012, 22, 19919.	6.7	189
179	Preparation of a three-dimensional interpenetrating network of TiO2 nanowires for large-area flexible dye-sensitized solar cells. RSC Advances, 2012, 2, 10550.	3.6	17
180	Morphology controllable fabrication of Pt counter electrodes for highly efficient dye-sensitized solar cells. Journal of Materials Chemistry, 2012, 22, 3948.	6.7	56

#	Article	IF	CITATIONS
181	High-temperature proton exchange membranes from ionic liquid absorbed/doped superabsorbents. Journal of Materials Chemistry, 2012, 22, 15836.	6.7	33
182	Facile Synthesis of Mesoporous Tin Oxide Spheres and Their Applications in Dye-Sensitized Solar Cells. Journal of Physical Chemistry C, 2012, 116, 20140-20145.	3.1	71
183	Redox-active alkaline electrolyte for carbon-based supercapacitor with pseudocapacitive performance and excellent cyclability. RSC Advances, 2012, 2, 6736.	3.6	140
184	Glucose Aided Preparation of Tungsten Sulfide/Multi-Wall Carbon Nanotube Hybrid and Use as Counter Electrode in Dye-Sensitized Solar Cells. ACS Applied Materials & Interfaces, 2012, 4, 6530-6536.	8.0	94
185	Template-free synthesis of a hierarchical flower-like platinum counter electrode and its application in dye-sensitized solar cells. RSC Advances, 2012, 2, 5034.	3.6	22
186	Alcohol elastomer based on superabsorbents. Polymers for Advanced Technologies, 2012, 23, 870-876.	3.2	0
187	Controllable hydrothermal synthesis of nanocrystal TiO2 particles and their use in dye-sensitized solar cells. Science China Chemistry, 2012, 55, 1308-1313.	8.2	11
188	Application of a novel redox-active electrolyte in MnO2-based supercapacitors. Science China Chemistry, 2012, 55, 1319-1324.	8.2	56
189	Low temperature fabrication of high performance and transparent Pt counter electrodes for use in flexible dye-sensitized solar cells. Science Bulletin, 2012, 57, 2329-2334.	1.7	10
190	Preparation of titanium dioxide-double-walled carbon nanotubes and its application in flexible dye-sensitized solar cells. Frontiers of Optoelectronics, 2012, 5, 224-230.	3.7	9
191	A Largeâ€Area Lightâ€Weight Dyeâ€Sensitized Solar Cell based on All Titanium Substrates with an Efficiency of 6.69% Outdoors. Advanced Materials, 2012, 24, 1884-1888.	21.0	146
192	Enhancement of the Photovoltaic Performance of Dyeâ€6ensitized Solar Cells by Doping Y <sub>0.78</sub> Yb <sub>0.20</sub> Er <sub>0.02</sub> F <sub>3</sub> in the Photoanode. Advanced Energy Materials, 2012, 2, 78-81.	19.5	131
193	Gelation of a liquid electrolyte with aniline for use in a quasi-solid-state dye-sensitized solar cell. Science China Chemistry, 2012, 55, 242-246.	8.2	5
194	Anhydrous proton exchange membrane operated at 200 °C and a well-aligned anode catalyst. Journal of Materials Chemistry, 2011, 21, 16010.	6.7	18
195	A facile route to a macroporous silver network for methanol oxidation. RSC Advances, 2011, 1, 1453.	3.6	10
196	A facile way to fabricate highly efficient photoelectrodes with chemical sintered scattering layers for dye-sensitized solar cells. Journal of Materials Chemistry, 2011, 21, 15552.	6.7	28
197	Flexible and macroporous network-structured catalysts composed of conducting polymers and Pt/Ag with high electrocatalytic activity for methanol oxidation. Journal of Materials Chemistry, 2011, 21, 13354.	6.7	37
198	Highly conducting multilayer films from graphene nanosheets by a spin self-assembly method. Journal of Materials Chemistry, 2011, 21, 5378.	6.7	24

#	Article	IF	CITATIONS
199	Facile secondary-template synthesis of polyaniline microtube array for enhancing glucose biosensitivity. Journal of Materials Chemistry, 2011, 21, 12927.	6.7	13
200	Application of Poly (3, 4-ethylenedioxythiophene): polystyrenesulfonate counter electrode in polymer heterojunction dye-sensitized solar cells. Frontiers of Optoelectronics in China, 2011, 4, 369-377.	0.2	4
201	Flexible solar cells based on PCBM/P3HT heterojunction. Frontiers of Optoelectronics in China, 2011, 4, 108-113.	0.2	6
202	Influence of surfactants on the morphology and photocatalytic activity of Bi2WO6 by hydrothermal synthesis. Science China Chemistry, 2011, 54, 211-216.	8.2	13
203	Flexible dye-sensitized solar cell based on PCBM/P3HT heterojunction. Science Bulletin, 2011, 56, 325-330.	1.7	38
204	Application of upconversion luminescence in dye-sensitized solar cells. Science Bulletin, 2011, 56, 96-101.	1.7	36
205	Preparation of porous nanoparticle TiO2 films for flexible dye-sensitized solar cells. Science Bulletin, 2011, 56, 2649-2653.	1.7	16
206	Preparation of Gd2O3:Eu3+ downconversion luminescent material and its application in dye-sensitized solar cells. Science Bulletin, 2011, 56, 3114-3118.	1.7	31
207	Quasiâ€solidâ€state dyeâ€sensitized solar cells containing P (MMAâ€ <i>co</i> â€AN)â€based polymeric gel electrolyte. Polymers for Advanced Technologies, 2011, 22, 1812-1815.	3.2	12
208	Oligomer ethylene glycol based electrolytes for dyeâ€sensitized solar cell. Journal of Applied Polymer Science, 2011, 120, 2786-2789.	2.6	1
209	Application of thermosetting organic solvent free polymer gel electrolyte in quasiâ€solidâ€state dyeâ€sensitized solar cell. Journal of Applied Polymer Science, 2010, 116, 1329-1333.	2.6	4
210	A multifunctional hydrogel with highâ€conductivity, pHâ€responsive, and release properties from polyacrylate/polyptrrole. Journal of Applied Polymer Science, 2010, 116, 1376-1383.	2.6	9
211	A highly efficient electric additive for enhancing photovoltaic performance of dye-sensitized solar cells. Science China Chemistry, 2010, 53, 1352-1357.	8.2	7
212	Preparation of sub-micron size anatase TiO2 particles for use as light-scattering centers in dye-sensitized solar cell. Journal of Materials Science: Materials in Electronics, 2010, 21, 833-837.	2.2	19
213	PF127 aided preparation of super-porous TiO2 film used in highly efficient quasi-solid-state dye-sensitized solar cell. Journal of Materials Science: Materials in Electronics, 2010, 21, 1000-1004.	2.2	6
214	Dye-sensitized solar cell with a solid state organic–inorganic composite electrolyte containing catalytic functional polypyrrole nanoparticles. Journal of Sol-Gel Science and Technology, 2010, 53, 599-604.	2.4	9
215	High conducting multilayer films from poly(acrylic acid) and graphite by layerâ€byâ€layer selfâ€assembly. Polymer Composites, 2010, 31, 145-151.	4.6	3
216	Preparation and electrical conductivity of SiO2/polypyrrole nanocomposite. Journal of Materials Science, 2009, 44, 849-854.	3.7	34

#	Article	IF	CITATIONS
217	Synthesis of polyacrylate/polyethylene glycol interpenetrating network hydrogel and its sorption for Fe3+ ion. Journal of Materials Science, 2009, 44, 726-733.	3.7	25
218	Preparation of porous polyacrylate/poly(ethylene glycol) interpenetrating network hydrogel and simplification of Flory theory. Journal of Materials Science, 2009, 44, 3712-3718.	3.7	29
219	Synthesis and properties of poly(acrylamideâ€ <i>co</i> â€acrylic acid)/polyacrylamide superporous IPN hydrogels. Polymers for Advanced Technologies, 2009, 20, 1044-1049.	3.2	10
220	Two steps synthesis and conductivity of polyacrylamide/Cu conducting hydrogel. Polymer Composites, 2009, 30, 1132-1137.	4.6	4
221	Synthesis of polyacrylate/poly(ethylene glycol) hydrogel and its absorption properties for heavy metal ions and dye. Polymer Composites, 2009, 30, 1183-1189.	4.6	26
222	Application of polymer gel electrolyte with graphite powder in quasiâ€solidâ€state dyeâ€sensitized solar cells. Polymer Composites, 2009, 30, 1687-1692.	4.6	14
223	Design and electrical conductivity of poly(acrylic acidâ€ <i>g</i> â€gelatin)/graphite conducting gel. Polymer Engineering and Science, 2009, 49, 1871-1878.	3.1	11
224	A multifunctional poly(acrylic acid)/gelatin hydrogel. Journal of Materials Research, 2009, 24, 1653-1661.	2.6	24
225	Synthesis of polyacrylate/polyethylene glycol interpenetrating network hydrogel and its sorption of heavy-metal ions. Science and Technology of Advanced Materials, 2009, 10, 015002.	6.1	47
226	Template-free synthesis of closed-microporous hybrid and its application in quasi-solid-state dye-sensitized solar cells. Energy and Environmental Science, 2009, 2, 524.	30.8	66
227	A simple route to high-strength hydrogel with an interpenetrating polymer network. E-Polymers, 2009, 9, .	3.0	2
228	Two-step synthesis of polyacrylamide/poly(vinyl alcohol)/polyacrylamide/graphite interpenetrating network hydrogel and its swelling, conducting and mechanical properties. Journal of Materials Science, 2008, 43, 5898-5904.	3.7	38
229	Two-step synthesis of polyacrylamide/polyacrylate interpenetrating network hydrogels and its swelling/deswelling properties. Journal of Materials Science, 2008, 43, 5884-5890.	3.7	39
230	The preparation and electrical conductivity of polyacrylamide/graphite conducting hydrogel. Journal of Applied Polymer Science, 2008, 108, 1490-1495.	2.6	26
231	Synthesis, characterization, and properties of polypyrrole/expanded vermiculite intercalated nanocomposite. Journal of Applied Polymer Science, 2008, 110, 2862-2866.	2.6	16
232	Progress on the electrolytes for dye-sensitized solar cells. Pure and Applied Chemistry, 2008, 80, 2241-2258.	1.9	234
233	Crystal Morphology of Anatase Titania Nanocrystals Used in Dye-Sensitized Solar Cells. Crystal Growth and Design, 2008, 8, 247-252.	3.0	83
234	An All-Solid-State Dye-Sensitized Solar Cell-Based Poly( <i>N</i> -alkyl-4-vinyl-pyridine iodide) Electrolyte with Efficiency of 5.64%. Journal of the American Chemical Society, 2008, 130, 11568-11569.	13.7	243

#	Article	IF	CITATIONS
235	Conducting Film from Graphite Oxide Nanoplatelets and Poly(acrylic acid) by Layer-by-Layer Self-Assembly. Langmuir, 2008, 24, 4800-4805.	3.5	90
236	Synthesis, characterization and properties of polyaniline/expanded vermiculite intercalated nanocomposite. Science and Technology of Advanced Materials, 2008, 9, 025010.	6.1	12
237	A high mechanical strength hydrogel from polyacrylamide/polyacrylamide with interpenetrating network structure by two-steps synthesis method. E-Polymers, 2008, 8, .	3.0	2
238	Fabrication and Photocatalytic Properties of HLaNb2O7/(Pt, Fe2O3) Pillared Nanomaterial. Journal of Physical Chemistry C, 2007, 111, 3624-3628.	3.1	43
239	Preparation and water absorbency of a novel poly(acrylate-co-acrylamide)/vermiculite superabsorbent composite. Journal of Applied Polymer Science, 2007, 104, 735-739.	2.6	45
240	Preparation of a novel polymer gel electrolyte based on N-methyl-quinoline iodide and its application in quasi-solid-state dye-sensitized solar cell. Journal of Sol-Gel Science and Technology, 2007, 42, 65-70.	2.4	18
241	Photocatalytic intercalated material based on HLaNb2O7 as host and Cd0.8Zn0.2S as guest. Science in China Series B: Chemistry, 2007, 50, 514-519.	0.8	9
242	Swelling behavior of poly(sodium acrylate)/kaoline superabsorbent composite. Polymer Engineering and Science, 2006, 46, 324-328.	3.1	14
243	Synthesis and photocatalytic properties of H2La2Ti3O10/TiO2 intercalated nanomaterial. Journal of Porous Materials, 2006, 13, 55-59.	2.6	12
244	Synthesis and Photocatalytic Properties of HTaWO6 Intercalated with Oxide Materials. Journal of Porous Materials, 2005, 12, 23-27.	2.6	4
245	Photocatalytic activities of layered intercalated materials H2NiTi4O10/TiO2 under UV and visible light irradiation. Materials Research Society Symposia Proceedings, 2005, 876, 1.	0.1	0
246	Preparation of a starch-graft-acrylamide/kaolinite superabsorbent composite and the influence of the hydrophilic group on its water absorbency. Polymer International, 2003, 52, 1909-1912.	3.1	50
247	Synthesis and photocatalytic properties of layered HNbWO6/(Pt, Cd0.8Zn0.2S) nanocomposites. Journal of Materials Chemistry, 2001, 11, 3343-3347.	6.7	58
248	Influence of the COOH and COONa groups and crosslink density of poly(acrylic) Tj ETQq0 0 0 rgBT /Overlock 10 T 50, 1050-1053.	ff 50 227 3.1	Td (acid)/mo 124
249	Synthesis and Properties of Poly(acrylic acid)/Mica Superabsorbent Nanocomposite. Macromolecular Rapid Communications, 2001, 22, 422-424.	3.9	253
250	Hydrothermal synthesis of HNbWO6/MO series nanocomposites and their photocatalytic properties. Journal of Materials Science, 2001, 36, 3055-3059.	3.7	10
251	Synthesis and Photochemical Properties of Semiconductor/Layered Compound Nanocomposites. International Journal of the Society of Materials Engineering for Resources, 2001, 9, 1-5.	0.1	0
252	Study on Bound Rubber in Silicone Rubber Filled with Modified Ultrafine Mineral Powder. Rubber Chemistry and Technology, 2000, 73, 19-24.	1.2	10

#	Article	IF	CITATIONS
253	Surface Energy of Mineral Powders and Interaction Between Silicone Rubber Matrix and Mineral Filler. Journal of Materials Science Letters, 1999, 18, 461-462.	0.5	11
254	Improvement of Quasi-Solid-State Supercapacitors Based on "Water-in-Salt―Hydrogel Electrolyte by Introducing Redox-Active Ionic Liquid and Carbon Nanotubes. New Journal of Chemistry, 0, , .	2.8	3
255	Potassium oleate as an effective interface modifier for defect passivation in planar perovskite solar cells. Functional Materials Letters, 0, , .	1.2	1